The Role of Active Site Residue Arginine 218 in Firefly Luciferase Bioluminescence†

Bruce R. Branchini,* Rachelle A. Magyar, Martha H. Murtiashaw, and Nathan C. Portier

Department of Chemistry, Connecticut College, New London, Connecticut 06320

Received September 25, 2000; Revised Manuscript Received December 5, 2000

ABSTRACT: Firefly luciferase catalyzes the highly efficient emission of yellow−green light from substrate firefly luciferin by a sequence of reactions that require Mg-ATP and molecular oxygen. We had previously developed a working model of the luciferase active site based on the X-ray structure of the enzyme without bound substrates. In our model, the side chain guanidinium group of Arg218 appears to be located in close proximity to the substrate's hydroxyl group at the bottom of the luciferin binding pocket. A similar role for Arg337 also has been proposed. We report here the construction, purification, and characterization of mutant luciferases R218A, R218Q, R218K, R337Q, and R337K. Alteration of the Arg218 side chain produced enzymes with 15−20-fold increases in the K_m values for luciferin. The contrasting near-normal K_m values for luciferin determined with the Arg337 enzymes support our proposal that Arg218 (and not Arg337) is an essential luciferin binding site residue. Bioluminescence emission studies indicated that in the absence of a positively charged group at position 218, red bioluminescence was produced. Based on this result and those of additional fluorescence experiments, we speculate that Arg218 maintains the polarity and rigidity of the emitter binding site necessary for the normal yellow−green emission of *P. pyralis* luciferase. The findings reported here are interpreted in the context of the firefly luciferase X-ray structures and computational-based models of the active site.

Bioluminescence—the conversion of chemical energy into light by a living organism—is beautifully illustrated by the flashing light produced by the firefly. Basic research mainly focused on the North American firefly *Photinus pyralis* (*1*−*3*) has progressed toward a very good understanding of the chemical transformations leading to light emission. The applications of firefly bioluminescence now include in vivo luminescence monitoring (*4*), as well as an impressive list of medical and pharmaceutical methods, many of which use the firefly luciferase gene as a reporter of gene expression and regulation (*5*−*7*).

As indicated in eqs 1−3 and Figure 1, the Luc[1] enzyme functions as a monooxygenase, although it does so without the apparent involvement of a metal or cofactor. By some means, amino acid residues are recruited to promote the addition of molecular oxygen to LH_2-AMP, which is then transformed to an electronically excited-state oxyluciferin molecule (Figure 1) and CO_2, both containing one oxygen atom from molecular oxygen (*1*, *8*). Relaxation of excited-state oxyluciferin to the corresponding ground state is accompanied by the emission of light. A quantum yield of ∼0.9 for this process (*9*) reflects not only an efficient catalytic machinery, but also a highly favorable environment for the radiative decay of an excited state. Firefly luciferase also catalyzes the in vitro formation of the adenylate of synthetic dehydroluciferin (L-AMP) (eq 4), an intermediate that cannot react further and potently inhibits Luc activity (*10*).

$$\text{Luc} + \text{LH}_2 + \text{ATP} \overset{\text{Mg}^{2+}}{\rightleftharpoons} \text{Luc·LH}_2\text{-AMP} + \text{PP}_i \quad (1)$$

$$\text{Luc·LH}_2\text{-AMP} + \text{O}_2 \rightarrow \text{Luc·oxyluciferin*} + \text{AMP} + \text{CO}_2 \quad (2)$$

$$\text{Luc·oxyluciferin*} \rightarrow \text{Luc·oxyluciferin} + h\upsilon \quad (3)$$

$$\text{Luc} + \text{L} + \text{ATP} \overset{\text{Mg}^{2+}}{\rightleftharpoons} \text{Luc·L-AMP} + \text{PP}_i \quad (4)$$

A particularly intriguing aspect of firefly bioluminescence encompasses the relationship between luciferase structure and light emission color. According to the original theory (*8*) based predominantly on studies of the *P. pyralis* enzyme, red light emission (λ_{max} 615 nm), which is observed at pH ∼6.0, results from the keto form of the emitter. At pH 7.8, the familiar yellow−green light emission (λ_{max} 560 nm) is produced from the enolate dianion form of the excited-state oxyluciferin by a presumed enzyme-assisted tautomerization (Figure 1, step f). In nature, beetle luciferases, which all

† This work was supported by a grant from the National Science Foundation (MCB 9816898) and the Hans & Ella McCollum-Vahlteich '21 Endowment.

* To whom correspondence should be addressed at the Department of Chemistry, Connecticut College, 270 Mohegan Ave., New London, CT 06320. Tel.: (860) 439-2479; Fax: (860) 439-2477; E-mail: brbra@conncoll.edu.

[1] Abbreviations: CB, 50 mM Tris-HCl (pH 7.0), 150 mM NaCl, 1 mM EDTA and 1 mM DTT.; GST, glutathione-S-transferase; Luc, *Photinus pyralis* luciferase (E. C. 1.13.12.7); LH_2, D-firefly luciferin; L, dehydroluciferin; LH_2-AMP, luciferyl-O-adenosine monophosphate; PheA, the phenylalanine-activating subunit of gramicidin synthetase 1; TICT, twisted intramolecular charge transfer; TNS, 6-*p*-toluidino-2-naphthalenesulfonic acid; WT, wild-type *Photinus pyralis* luciferase containing the additional N-terminal peptide GPLGS.

10.1021/bi002246m CCC: $20.00
Published on Web 01/30/2001

utilize the same firefly luciferin substrate, display various colors of light from green (λ_{max} ~530 nm) to red (λ_{max} ~635 nm) (*11, 12*).

Color modulation has also been attributed to alterations in firefly luciferase structures resulting in changes of polarity (*13*) or rigidity (*14, 15*) of the emitter binding site. In the latter theory (*14, 15*), conformations of the keto form of oxyluciferin, related by rotation about the C2−C2′ bond (Figure 1), account for the color variation. Red emission is attributed to the minimum energy conformation of an unusual twisted intramolecular charge transfer (TICT) excited state (Figure 1) in which the aromatic rings of oxyluciferin are rotated 90° about the C2−C2′ bond. Yellow−green light emission would result from a higher energy excited-state conformer. The proposed mechanisms for bioluminescence color have been reviewed (*2, 16*).

The cloning and sequencing of *P. pyralis* luciferase and similar enzymes from 12 other beetle species[2] (*17*−*20*) have revealed that these luciferases are closely related to a large family of nonbioluminescent proteins (*21, 22*) that catalyze reactions of ATP with carboxylate substrates to form acyl-adenylates. The formation of enzyme-bound LH_2-AMP and L-AMP (eqs 1 and 4) illustrates one step of the common chemistry. The "acyl-adenylate/thioester-forming" superfamily of enzymes (*23*) includes the following: a variety of acyl:CoA ligases; the acyl-adenylate-forming domains of enzyme complexes involved in the nonribosomal synthesis of peptides and polyketides (*23*); the luciferases; and several other types of enzymes. Most of these enzymes generate thioester (e.g., of CoA) intermediates or products from the initially formed corresponding acyl-adenylates; these reactions are similar to one suggested (*24*) to account for the stimulatory effect of CoA on Luc activity.

The Luc crystal structure without bound substrates (*25*), the first structure of a member of the "acyl-adenylate/thioester-forming" enzyme family (*23*), revealed a unique molecular architecture consisting of a large N-terminal domain (residues 1−436) and a small C-terminal domain (residues 440−550). Based on an analysis of the positions of approximately seven strictly conserved residues among a group of enzymes sharing the adenylation function, a general location of the Luc active site was proposed (*25*). Many of these invariant residues were found on the surfaces of the two Luc domains opposite to each other and separated by a wide solvent cleft (*25*). Next, the crystal structure of a second member of the adenylate-forming family, the phenylalanine-activating subunit of gramicidin synthetase 1 (PheA) in a complex with phenylalanine, Mg ion, and AMP, was reported (*26*). The active site of PheA was determined to be at the interface of the two domains, which were remarkably similar in size and shape to the corresponding domains of Luc. In the PheA structure, however, the C-terminal domain was rotated 94° and was 5 Å closer to the N-terminal domain than in the "open" Luc structure (*26*). Starting with the crystal structures of Luc (*25*) and PheA (*26*), we used molecular modeling techniques to produce a potential working model (Figure 2) of the Luc active site containing substrates LH_2 and Mg-ATP (*27*). Subsequently, the crystal structure of Luc containing two molecules of bromoform, a general anesthetic and Luc inhibitor, was described (*28*). One of the bromoform molecules binds in a site tentatively identified as the LH_2 binding pocket, based on the location of the phenylalanine binding site in the PheA structure (*26, 28*). Additionally, a model of the Luc−ATP−LH_2 complex (*29*) produced by molecular modeling and energy minimization provides another concept of the Luc active site. While both models (*28, 29*) describe a Luc site of LH_2 binding that is in very good general agreement with our proposal (*23*), there are differences, particularly in the locations of Arg218 and Arg337. We therefore undertook the present mutational and biochemical studies of Arg218 and Arg337 directed at determining the functions of these residues in beetle bioluminescence.

MATERIALS AND METHODS

Materials. The following items were obtained from the indicated sources: Mg-ATP (equine muscle) (Sigma); LH_2 (Biosynth AG); restriction endonucleases, T4 polynucleotide kinase, and T4 DNA ligase (New England Biolabs); and mutagenic oligonucleotides (Genosys). LH_2-AMP was synthesized according to the method of Morton et al. (*13*), purified by reversed-phase high-performance liquid chromatography (*30*), and stored at −70 °C as a lyophilized solid. Dehydroluciferin (L) was prepared as described by a literature method (*8*). WT and mutant luciferases containing the additional N-terminal peptide GPLGS- were constructed and purified as GST-fusion proteins as previously reported (*27, 31*).

General Methods. Detailed procedures including descriptions of the equipment used to determine bioluminescence activity of the luciferases by flash height- and integration-based light assays have been described previously (*27, 31, 32*). The procedures, equipment, and methods reported earlier (*27, 31*−*33*) were used to obtain the following: fluorescence emission spectra; pH optima; steady-state kinetic constants for LH_2, LH_2-AMP, and Mg-ATP; bioluminescence emission spectra; circular dichroic spectra; and total protein. Mass spectral analyses of the Luc proteins were performed by tandem HPLC-electrospray ionization mass spectrometry using a Perkin-Elmer Series 200 HPLC system and a Sciex ABI150A mass spectrometer. The Luc proteins used in this study had molecular masses (WT, 61 155; R218K, 61 129; R218Q, 61 128; R218A, 61 072; R337K, 61 128; and R337Q, 61 128 Da) within ±2 mass units of the calculated values.

Site-Directed Mutagenesis. To produce the mutant luciferase proteins, mutagenesis of WT in the pGex-6P-2 vector was performed with the Chameleon double-stranded mutagenesis kit (Stratagene) using *Alwn*I as the selection endonuclease. Site-directed mutagenesis was carried out according to the manufacturer's instructions using the following primers: R218K, 5′-CTTCCGCATCGGACCGCCTGCGTC**AAA**TTCTCGCA-3′ [*Rsr*II]; R218Q, 5′-CTTCCGCATCGGACCGCCTGCGTC**CAA**TTCTCGCA-3′ [*Rsr*II]; R218A, 5′-CTTCCGCATCGGACCGCCTGCGTC**GCA**TTCTCGCA-3′ [*Rsr*II]; R337K, 5′-TCCATCTTCCCGGGATA**AAA**CAAGGATATGG-3′ [*Sma*I]; R337Q, 5′-TCCATCTTCCCGGGATA**CAA**CAAGGATATGG-3′ [*Sma*I] (where underlines represent silent changes to create unique screening endonuclease sites, boldface represents the mutated codons, and

[2] The deduced amino acid sequence of *Phengodes species* luciferase was provided by K. V. Wood and M. Gruber, personal communication.

Table 1: Bioluminescent Activity of Luciferase Enzymes

enzyme	relative specific activity[a]		rise time[b]	decay time[b]	pH[b]	bioluminescence[c]
	flash height	integrated	(s ± 0.15)	(min ± 0.01)	optima	emission max (nm)
WT	100.0	100.0	0.50	0.20	8.2	557 (62)
R218K	33.0	165.0	0.62	7.02	8.0	572 (69)
R218Q	5.1	40.5	0.99	4.85	8.0	608 (74)
R218A	3.6	30.0	1.21	4.35	8.0	611 (84)
R337K	40.6	49.5	0.41	0.12	8.2	595 (64)
R337Q	3.3	20.5	0.51	0.90	7.2	594 (65)

[a] Specific activity measurements were made as previously described (*27, 31, 32*). WT values are defined as 100.0 and are equivalent to 1.18×10^{15} photons s^{-1} mg^{-1} (0.12 einstein $\times 10^{-6}$ s^{-1} μmol^{-1}) and 2.45×10^{16} photons mg^{-1} (2.5 einstein $\times 10^{-6}$ μmol^{-1}) for flash height-based and 15 min integration-based assays, respectively. In the standard activity assays, the final concentrations of Mg-ATP and LH_2 were 2 mM and 70 μM, respectively. For mutants with elevated K_m values, substrate concentrations were adjusted: R218K, 400 μM LH_2; R218Q, 8.0 mM Mg-ATP and 750 μM LH_2; R218A, 14 mM Mg-ATP and 750 μM LH_2; and R337Q, 10 mM Mg-ATP. All R337Q activity assays were performed at pH 7.2. Light intensity data were corrected for the spectral response of the Hamamatsu 931B photomultiplier tube and differences in the bandwidths of the emission spectra (*27, 31*). The error associated with the specific activity measurements is ±10% of the value. [b] Measurements performed as previously described (*27, 31, 33*). [c] Bioluminescence emission spectra of all enzyme-catalyzed reactions were measured at pH 7.8 as described earlier (*31*) except R337Q, which was evaluated at pH 7.2. Bandwidths (nm) at 50% of emission maxima are indicated in parentheses.

brackets indicate the screening endonucleases used). The primer 5′-TCCTGTTACCAGTCGCGACTGCCAGTG-3′ [*Nru*I] was included in each mutagenesis reaction to introduce an *Alwn*I selection site.

Kinetic Constants for Luc Inhibitors. The reversible inhibition of WT and the mutant enzymes by L and TNS (Figure 3) was assessed with respect to LH_2 using assay conditions and methods reported earlier (*34*). The initial velocities of the enzyme-catalyzed light reactions were determined as a function of LH_2 concentration (4−600 μM) in the presence or absence of the inhibitor. Mg-ATP was present at saturating concentration in each study. Inhibitor concentrations of 0.1−40 μM (L) and 7.0−135 μM (TNS) were used. Inhibition constants (K_i) for each inhibitor with the Luc enzymes were determined by the method of Dixon (*35*).

Effect of Arg218 Mutations on the Fluorescence of Luc−L and Luc−TNS Complexes. It has previously been demonstrated (*36, 37*) that the formation of a Luc−L complex could be monitored by the enhancement of the 440 nm fluorescence emission of L, which is very weak in the absence of enzyme. Using an excitation wavelength of 350 nm, the fluorescence emission spectra (390−650 nm) of 30 μM solutions of L in 50 mM Tris buffer, pH 7.4, were recorded before and after the addition of WT or the Arg218 mutant enzymes (5.5 μM final concentration). A concentration of 30 μM L was used to ensure formation of enzyme−L complexes with the mutants. At this concentration of L, there was no evidence of an inner filter effect (*38*).

Concurrent with the formation of a Luc−TNS complex, a new fluorescence emission peak appears at 425 nm (*39*). Using an excitation wavelength of 350 nm, the fluorescence emission spectra (390−550 nm) of 10−100 μM solutions of TNS in 50 mM Tris buffer, pH 7.4, were recorded before and after the addition of enzymes (1.0 μM final concentration). The concentrations of TNS used with the Arg218 mutants were adjusted to ensure complete enzyme−TNS complex formation. With TNS concentrations greater than 10 μM, it was necessary to apply a correction for an inner filter effect (*38*).

Fluorescence-Based Measurement of the Chemical Denaturation of the Luc Enzymes. The unfolding of the Luc enzymes was monitored by measuring protein Trp residue fluorescence in the presence of guanidinium chloride as described by Frydman (*40*). Stock enzyme solutions were exchanged by extensive dialysis into 20 mM HEPES−KOH containing 100 mM potassium acetate, 5 mM magnesium acetate, 0.5 mM EDTA, and 1 mM DTT. Protein solutions (57 μg/mL) containing varying concentrations of guanidinium chloride (0.1−6.0 M) were incubated at 25 °C for 1 h. Fluorescence emission spectra were recorded over the range 300−400 nm with excitation at 295 nm.

RESULTS

Overexpression, Purification, and Characterization of Luc Proteins. WT and the mutant luciferases listed in Table 1 were expressed as GST-fusion proteins and contained the additional N-terminal peptide GPLGS- (*27, 31*), which remained after protease cleavage of GST. Average yields of purified WT, R218K, R218Q, R218A, R337K, and R337Q were 16, 6, 9, 4, 2, and 1 mg/L of culture volume, respectively. All proteins were purified to homogeneity as judged by sodium dodecyl sulfate−polyacrylamide gel electrophoresis and reversed-phase HPLC (data not shown). The enzymes remained fully active for up to 6 months on storage at 4 °C, except the R337Q protein, which lost 20% activity over 2 weeks. The R337Q protein was characterized within 2 weeks of purification; however, due to the relative instability of this enzyme, all parameters were not assessed.

The tertiary structures of the mutants appeared to be very similar to that of WT as assessed by nearly superimposable protein Trp residue fluorescence emission spectra measured in the presence of increasing concentrations of guanidinium chloride (data not shown). Notably, increasing the denaturant concentration above 250 mM resulted in dramatic fluorescence decreases (monitored at 336 nm) for the WT and all mutants as had been reported (*40*) for native Luc. The far-UV circular dichroic (CD) spectra (data not shown) of the Arg218 mutants, the R337K protein, and WT were nearly indistinguishable, indicating that the mutations had little, if any, effect on secondary structure.

Bioluminescence Activity of the Luciferases. Our previously proposed working model (*27*) of the Luc active site suggested that only the side chain groups of His245, Thr343, and Lys529 are within 6 Å of the C4 or C5 atoms of LH_2 (Figure 1). Additionally, the model indicated that Arg218 is proximal to the 6′-hydroxyl group of LH_2 (Figure 2). Many

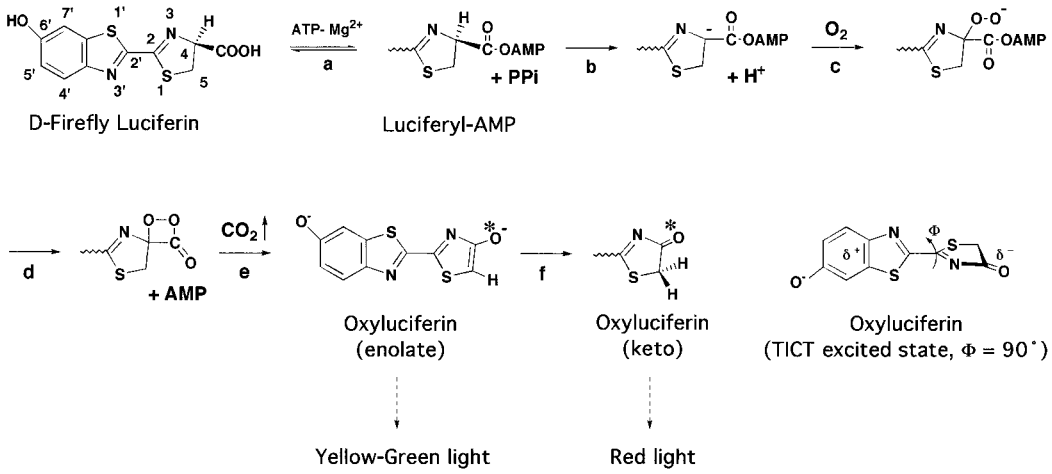

FIGURE 1: Mechanism of Luc-catalyzed bioluminescence and the chemical structure of the TICT excited state of oxyluciferin.

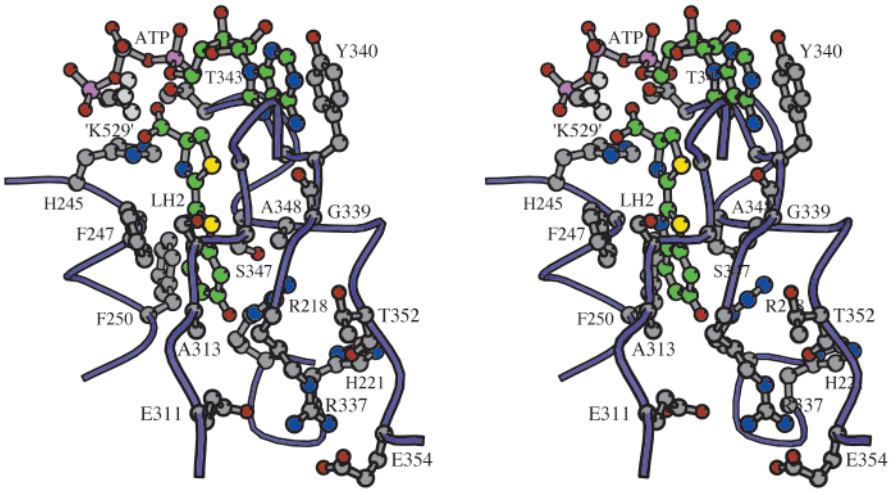

FIGURE 2: Stereo diagram showing the substrate binding sites suggested (*27*) by molecular modeling of Luc with LH_2 and ATP (carbon atoms are green in both) and Mg^{2+} ion (not shown). The model was created starting with the Luc X-ray structure 1LCI (*25*), and methylammonium ion (labeled 'K529') was used to represent possible interactions of the Lys529 side chain. Traces through the α-carbons of regions V217−H221, H244−T252, H310−L319, and R337−G355 are shown as purple coils. The α-carbons of G246, S314 (and side chain group), G315, G316, and G341 are shown (gray) but are not labeled. The main chain carbonyl groups (oxygen atoms are red) of G339 and T352 also are shown. This diagram was generated using the program MOLSCRIPT (*45*).

of the Luc enzymes with mutations at His245 and Thr343 displayed longer wavelength bioluminescence emission than WT, and these residues were shown to have significant roles in the determination of bioluminescence color (*31*). In contrast, all Lys529 mutants have emission maxima very similar to WT (*31*, *32*). The Arg337 mutations led to a 38 nm shift in bioluminescence emission to longer wavelength, and the Arg218 mutant spectra were red-shifted 15−54 nm (Table 1 and Figure 4).

Specific activities for all luciferases were measured, corrected for differences in the colors and shapes of their emission spectra (*31*), and expressed as flash height- and integration-based values (Table 1). The former values relate the maximum achievable overall reaction rate for the combined adenylation and oxidation steps (eqs 1−3). The relative values presented in Table 1 are comparisons of the mutant enzymes to WT. Among the Arg218 mutants, the conservative substitution Arg to Lys resulted in a slightly lower (~3-fold) flash height-based specific activity. The loss of the positively charged side chain was more deleterious; the R218Q and R218A mutants had 20-fold and 28-fold reduced specific activities, respectively (Table 1). The specific activities of the R337K and R337Q mutants were reduced 2.5- and 30-fold, respectively (Table 1).

Integrated specific activity values (photons/mg) were determined from estimates of the total light output in bioluminescence assays conducted under optimum conditions for each enzyme as specified in Table 1. The major differences in the time dependence of bioluminescence intensity among the Luc enzymes were prolonged emission profiles of the Arg218 mutants (Table 1). The integration-based specific activities of all of the mutant Luc enzymes listed in Table 1 were greater than the corresponding flash height-based ones, mainly due to the prolonged emission of light.

Effects of Luc Mutations on Substrate Binding and Catalytic Constants. To evaluate the effects of substitutions at positions 218 and 337 on the kinetic behavior of Luc, the steady-state kinetic parameters for the WT and mutant luciferases were determined (Table 2). Alteration of the Arg218 side chain led to a dramatic 15−20-fold increase in the K_m values for LH_2. In contrast, the changes at the Arg337 side chain had little, if any, effect on the K_m values for LH_2. The conservatively changed R218K and R337K luciferases

Table 2: Steady-State Kinetic Constants for Luciferase Enzymes

	K_m (μM)[a]			K_i (μM)[c]
enzyme	luciferin	Mg-ATP	k_{cat} (s^{-1})[b]	dehydroluciferin
WT	15	160	0.1250	0.15
R218K	217	690	0.0300	4.0
R218Q	304	3900	0.0081	12.5
R218A	301	6200	0.0040	9.5
R337K	14	200	0.0510	nd
R337Q	19	700	0.0036	nd

[a] Kinetic constants were determined as described (*31*, *32*). The error associated with K_m values falls within ±10% of the value. [b] V_{max} values determined with each enzyme were expressed in units of einstein × 10^{-6} s^{-1}. The corresponding k_{cat} values were obtained from the data used to determine the K_m values for LH_2 by dividing the V_{max} values by the final amount (μmol) of each enzyme in the assay mixtures. The error associated with these measurements falls within ±15% of the value. [c] L was evaluated as a reversible inhibitor of the luciferases with respect to LH_2 as described under Materials and Methods. Inhibition constants (K_i) were determined by the method of Dixon (*35*). The error associated with these values falls within ±15% of the value. Data not determined (nd).

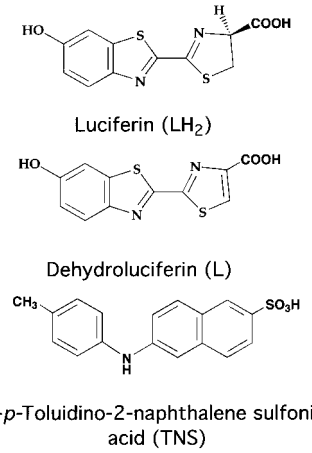

FIGURE 3: Chemical structures of firefly luciferin and related inhibitors.

had moderately elevated K_m values for Mg-ATP, as did R337Q. However, elimination of the positively charged side chain of Arg218 substantially increased the K_m values for Mg-ATP 24−38-fold (Table 2).

The k_{cat} values for all Luc mutants reflected the pronounced differences in overall flash height-based specific activities (Tables 1 and 2). The flash height-based values shown in Table 1 and the k_{cat} values in Table 2 are both based on the same maximal rate of the overall reaction (eqs 1−3 and Figure 1).

Noting the pronounced effects on the K_m values for LH_2 caused by mutations at Arg218, but not Arg337, we focused our investigations on the relationship of Arg218 to the integrity of the LH_2 binding site using L and the fluorescent dye TNS (Figure 3). These compounds were competitive, reversible inhibitors of WT (*36*, *37*, *39*) and the Arg218 mutants (Table 2). With the R218K mutant, 15−25-fold increases in both K_m for LH_2 and K_i for L were observed. The changes to Gln and Ala at position 218 resulted in additional 1.4−3-fold increases in K_m and K_i values relative to those obtained for LH_2 and L, respectively, with the R218K enzyme (Table 2).

An additional qualitative assessment of the LH_2 binding site of the Arg218 mutants was made by measuring their ability to enhance the intensity of the 440 nm fluorescence emission of L. This fluorescence change is associated with the formation of a Luc−L complex (*32*, *36*). With excitation at 350 nm, solutions of L alone display a very weak emission at 440 nm and an intense band at 550 nm, presumably representing the respective un-ionized and ionized phenolate transitions (*36*). WT and the Arg218 mutants variably enhanced the 440 nm fluorescence emission band of L, while the intensity of the 550 nm peak remained unchanged. The fluorescence intensities of the Arg218 mutant−L complexes at 440 nm were only ∼25% (R218K) and ∼10% (R218Q and R218A) of the value of the WT−L complex (data not shown). This protein-induced fluorescence enhancement that accompanies enzyme−L complex formation is thought to be due to an increase in the quantum yield of the emission of the small fraction of un-ionized (phenol form) L molecules (*36*).

Table 3: Apparent Kinetic Properties of Luciferase Enzymes with Synthetic LH_2-AMP[a]

enzyme	K_m (μM)	k_{cat} (s^{-1})	rise time[b] (s ± 0.15)	decay time[b] (min ± 0.01)
WT	3.4	0.178	0.40	0.02
R218K	4.1	0.128	0.24	0.14
R218Q	6.6	0.026	0.38	0.08
R218A	3.3	0.017	0.38	0.02
R337K	5.0	0.079	0.25	0.02
R337Q	5.1	0.005	0.40	0.02

[a] Kinetic constants were determined for enzyme-catalyzed bioluminescence reactions initiated with synthetic LH_2-AMP as previously described (*32*). The error associated with K_m and k_{cat} values falls within ±10% of the value. [b] Measurements performed as previously described (*32*). Bioluminescence decay times (to 20% of initial activity) were measured from maximum initial flash heights.

Similar fluorescence studies were conducted with TNS, a dye that has been used to examine the hydrophobicity of substrate binding sites in proteins (*41*), including Luc (*39*). With excitation at 350 nm, solutions of TNS fluoresce extremely weakly in the range 390−550 nm. The addition of Luc produces a strong emission band with a maximum at 425 nm (*39*). For each of the Arg218 mutants, increases in fluorescence intensity similar to WT were observed. The emission maxima, however, were shifted to 430 nm for R218K and to 438 nm for R218Q and R218A.

Effects of Mutations on the Luc Oxidative Partial Reaction. Measurements of the kinetic properties of WT and the Luc mutants with synthetic LH_2-AMP were undertaken to evaluate the effects of the amino acid changes on the Luc-catalyzed oxidative chemistry (eqs 2 and 3) after and independent of the rate of adenylate formation (eq 1). The light emission profiles (rise and decay times) of all the luciferase mutants with the preformed adenylate were similar (Table 3) to WT. The extended decay times of the Arg218 mutants that had previously been observed were greatly reduced when LH_2-AMP was substituted for substrates LH_2 and Mg-ATP (Table 1). Using the k_{cat} values for the enzyme-catalyzed production of bioluminescence from LH_2-AMP (Table 3), we estimated the rates of the oxidation reactions (eqs 2 and 3) for the Luc mutants. The relative rates for the Arg337 mutants with LH_2-AMP were nearly identical to the relative rates of the overall reactions with the natural substrates. In contrast, the relative rates of light production from synthetic LH_2-AMP with the Arg218 mutants were ∼3-

fold greater than their relative rates of overall light production with LH_2 and Mg-ATP.

DISCUSSION

Related Previous Studies. We had previously developed (*27*) a working model of the Luc active site (Figure 2) to aid in the design and interpretation of mutational studies with Luc. We subsequently used the model to examine the roles of putative Luc active site residues in the catalysis of the reactions leading to light emission (*27*, *32*) and in the determination of bioluminescence color (*31*). We initially focused our efforts on residues His245 and Thr343, the former being identified by site-directed photoinactivation studies as the key target of singlet oxygen-based enzyme inactivation (*27*, *34*). We were unable, however, to demonstrate a significant role for His245 in substrate binding or catalysis. In contrast, it is likely that Thr343, part of the adenylate-forming family motif II (*23*) (^{340}YGTE^{344} in Luc), does contribute to binding both substrates and to the catalysis of both Luc partial reactions (eqs 1−3). Moreover, although we could not clearly distinguish among the three prevalent theories of bioluminescence color (*2*, *8*, *13*−*16*), we did establish that His245 and Thr343 are critically important residues for the normal yellow−green bioluminescence of Luc (*31*).

Due to limitations in the size of the searched conformational space, the Luc C-terminal domain was not included in our molecular model. Instead, our calculations included the methylammonium ion to mimic the potential interactions of the side chain ammonium ion of Lys529 (Lys517 in PheA), an important active site residue in the analogous C-terminal domain of PheA (*26*). Our model shows the methylammonium ion is positioned near ATP and the carboxylate of LH_2 (Figure 2). A recent mutagenesis study (*32*) provided supporting results suggesting that Lys529 in Luc is a critical residue for effective substrate orientation and that it makes electrostatic interactions that are important for efficient adenylate production. Lys529 does not, however, have a significant role in the Luc-catalyzed oxidation reaction or in bioluminescence color determination.

One of the few constraints applied in the development of our model restricted the side chain guanidinium group of Arg218 to be within H-bonding distance of the phenolate ion of LH_2 (*27*). This interaction is apparent in Figure 2, where the side chain guanidinium group of Arg218 appears to anchor the benzothiazole ring of LH_2 in the LH_2 binding pocket through H-bonding interactions with the phenolate group. The main chain carbonyl of Ala348 and the side chain hydroxyl of Ser347 are also shown within H-bonding distance of Arg218. The modeling studies of Sandalova and Ugarova (*29*), however, suggest that both Arg218 and Arg337 are at the Luc active site and serve to shield the LH_2 hydroxyl group from solvent. In this model, only the guanidinium ion of Arg337 is shown to be within H-bonding distance of the LH_2 hydroxyl group. In a third model proposed by Brick and co-workers (*28*), a putative Luc binding site for LH_2 is shown near the site of a bound bromoform molecule in an X-ray structure reported recently. In this model (*28*), the charged Arg218 side chain is located on one side of the LH_2 binding pocket and is coordinated to four water molecules. The base of the binding pocket is comprised of the aliphatic chain of Arg337 while its guanidinium ion is H-bonded to the side chain carboxylate of Glu311 and the main chain carbonyl groups of Gly228 and Thr352. A second molecule of bound bromoform in the X-ray structure is positioned in a very polar environment near Glu311, Thr352, Glu354, His310, and the Arg337 side chain group. This "external site" is proximal to the LH_2 binding pocket (*28*), and its function is not known. Although the Arg337 guanidinium group in our model is predicted to be similarly near residues Gly228, Glu311, and Thr352, the aliphatic chain of Arg337 is not in the LH_2 binding pocket (Figure 2).

Interpretation of Kinetic Results. The elevated K_m values of the Arg218 mutants for LH_2 and contrasting near-normal values of the Arg337 mutant enzymes (Table 2) provide strong support that Arg218, and not Arg337, is an essential LH_2 binding site residue. Arg218 is absolutely conserved among all known beetle luciferases (*17*−*21*) (Figure 5), and even the conservative Arg to Lys substitution produces a protein with an ∼15-fold elevated K_m for LH_2. Among Luc mutants in which His245, Thr343, and Lys529 were changed, only the K529A protein had a similarly increased K_m value, which was attributed to the likely loss of an electrostatic interaction with the carboxylate of LH_2 (*32*). It is likely that the greater steric bulk and/or larger polar area of the Arg side chain accounts for the inability of even the R218K enzyme to bind LH_2 normally. If, as our model predicts, direct H-bonding interactions between the guanidinium side chain are essential for productive LH_2 binding, the R218K mutant may substitute poorly for this function because of an altered side chain conformation.

In 2 of the 20 available beetle luciferase sequences (*17*−*21*), Ile and Leu replace Arg at position 337 (Figure 5). The substitution of these large hydrophobic residues for Arg337 would be expected to be well tolerated if the position 337 residue simply provided steric bulk to make up the base of the LH_2 binding site. It seems unlikely, however, that the R337Q mutant, with its shorter aliphatic side chain, would bind LH_2 normally as the K_m value of this mutant for LH_2 indicates. Our experimental data and the luciferase sequence comparison information do not lend support to the proposal that Arg337 forms the base of the LH_2 binding pocket or that this residue is H-bonded to LH_2.

The removal of the positively charged side chain group of Arg218 had a pronounced deleterious effect on the binding of Mg-ATP that was not observed with R218K and the Arg337 mutants, as judged by the measured K_m values for Mg-ATP (Table 2). Possibly, with the R218Q and R218A enzymes, the adenine binding sites are disrupted by the loss of H-bonding interactions to Ser347 and Ala348, residues that in turn interact with the adenylate-forming family motif II binding residues Tyr340 and Leu342 (Figure 2).

The results of specific activity k_{cat} measurements (Tables 1 and 2) do not support significant roles for either Arg218 or Arg337 in the overall catalysis of light production. By substituting synthetic LH_2-AMP for LH_2 and Mg-ATP and by monitoring the light emission from bioluminescence reactions catalyzed by WT and the mutant luciferases, we determined the steady-state k_{cat} values (Table 3) for the overall oxidation processes (eqs 2 and 3). Since the relative rates for the Arg337 mutants with LH_2-AMP were nearly identical to the relative rates of the overall reactions with

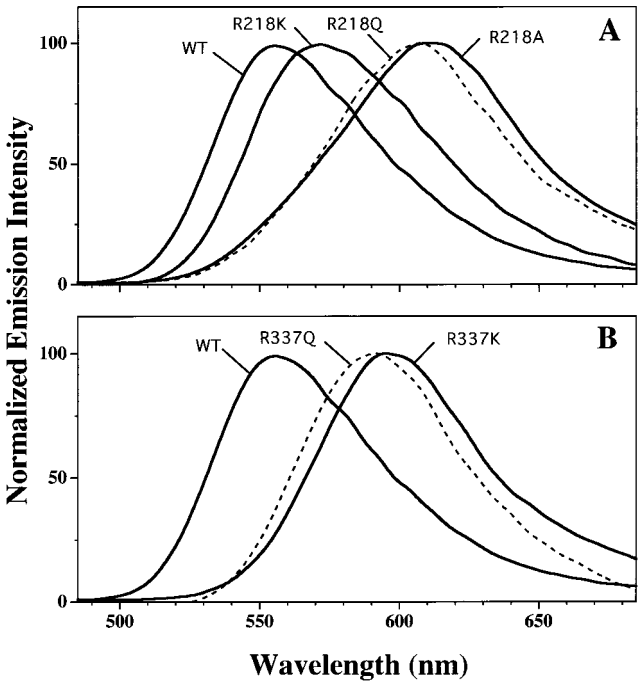

FIGURE 4: Bioluminescence emission spectra of WT and the Arg218 (panel A) and Arg337 mutants (panel B) at pH 7.8. The conditions used for recording and correcting the emission spectra are described in ref *31*.

the natural substrates, it is likely that changes at this position affect only the oxidative steps and not the adenylation reaction (eq 1). For the Arg218 mutants, a comparison of the k_{cat} values for the overall reactions with those using only the synthetic adenylate suggests that decreases in both the adenylation and oxidation processes are a consequence of the amino acid changes. The total light yields, which are independent of the rate of photon production, were not significantly reduced for the mutants examined (Table 1). The observed differences may be due to dark reactions that compete with the formation of product oxyluciferin, the yield of oxyluciferin in its excited state, and the efficiency of the radiative decay of the excited-state product.

Since it is reasonable to expect that oxyluciferin is made in the LH_2 binding site, we considered the possibility that one role of the positively charged Arg218 side chain is to make an electrostatic interaction important for ground-state ionization of the LH_2 phenol (pK_a ~8.7) and/or for stabilization of the excited-state phenolate ion (pK_a ~−1) of the oxyluciferin emitter. Both processes are thought to be important to ensure the high bioluminescence quantum yield of Luc (*13*). Suggestive evidence supporting this role for Arg218 includes the greater relative integrated light yields (Table 1) recorded with the mutant enzymes containing basic groups at position 218 compared to those with Gln and Ala.

Roles of Arg218 and Arg337 in Bioluminescence Color. The bioluminescence emission spectra of all the Arg218 and Arg337 mutant luciferases were red-shifted (Table 1 and Figure 4). This result is by no means unique, as there are at least 40 examples of single point mutants of various luciferases whose emission spectra are red-shifted with respect to their normal emissions (*2, 17, 31, 42*). While changes at residues likely to be at or very near the LH_2 binding pocket, e.g., His 245 and Thr343 in *P. pyralis* and Ser247 (Phe250 in Luc) in *P. plagiophthalamus*, have been shown to elicit color shifts (Figure 5), there are even more examples of remote residues causing alterations in emission color. Changes at remote residues are generally thought to

Beetle Luciferases	Emission (nm)	Selected Sequence Alignment				
Photinus pyralis (46)	557	^{218}**R**	^{245}**HGF**GMF^{250}	^{284}S	^{310}**HE**^{311}	^{337}RQ**GYGLTE**TTS**A**ILITPE^{354}	^{529}**K**
Lampyris noctiluca (47)	547	R	HGFGMF	S	HE	RQGYGLTETTSAIIITPE	K
Pyrocoelia miyako (48)	548	R	HVFQMF	S	HE	RQGYGLTETTSAIIITPE	K
Hotaria parvula (48)	548	R	HGFGMF	S	TE	RQGYGLTETTSAFIITPE	K
Luciola lateralis (49)	548	R	HGFGMF	S	VE	RQGYGLTETTSAIIITPE	K
Luciola lateralis(g) (50)	548	R	HGFGMF	S	VE	RQGYGLTETTSAIIITPE	K
Luciola cruciata (51)	562	R	HGFGMF	S	VE	RQGYGLTETTSAIIITPE	K
Luciola mingrelica (52)	570	R	HGFGMF	S	TE	RQGYGLTETTSAFIITPE	K
Photinus pennsylvanica(LY) (18)	545	R	HGFGMT	S	KE	RQGYGLTETTSAVLITPD	K
Photinus pennsylvanica(J19) (18)	552	R	HAFGTF	S	HE	RQGYGLTETTCAIVITAE	K
Photinus pennsylvanica1 (18)	552	R	HAFGTF	S	HE	RQGYGLTETTCAIVITAE	K
Photinus pennsylvanica2 (18)	545	R	HGFGMT	S	KE	RQGYGLTETTSAVLITPD	K
Pyrophorus plagiophthalamus							
Green *(17)*	546	R	HAFGFS	S	RE	RCGFGLTESTSANIHSL-	K
Yellow-green *(17)*	560	R	HAFGFS	S	RE	RCGFGLTESTSANIHSL-	K
Yellow *(17)*	578	R	HAFGFS	S	RE	RCGFGLTESTSANIHSL-	K
Orange *(17)*	593	R	HAFGFG	S	RE	RCGFGLTESTSANIHSL-	K
Phengodes[2]	549	R	HAFGMF	T	KE	IQGYGLTETCCAVLITPH	K
Pyrearinus termitilluminans (20)	538	R	HAFGFS	S	AE	RCGYGLTESTSANIHTLH	K
Phrixothrix vivianii (19)	548	R	HAFGMF	T	TE	IQGYGLTETCCAVMITPH	K
Phrixothrix hirtus (19)	623	R	HAFGLF	S	TE	LQGYGLTETCSALILSPN	K

FIGURE 5: Deduced amino acid sequence comparison of selected regions of the beetle luciferases. The emission wavelength entries are the reported bioluminescence emission maxima for reactions catalyzed by each enzyme. Amino acids in boldface type are conserved among all beetle luciferases. Within the selected regions shown, mutations of beetle luciferases have been reported at the following positions (*P. pyralis* numbering): R218 (*43*), H245 (*27, 31*), S284 (*42, 53*), T343 (*31*), E354 (*54*), and K529 (*31, 32*).

exert long-range effects through the alteration of polypeptide packing that, in turn, modifies the structure of the Luc active site. Changes in binding site polarity, positioning of key side chain nucleophiles, and the rigidity of the binding sites for substrates and emitter may account for the color differences (*2, 16*). We speculate that the color shifts evoked by the Arg337 changes result from alterations in the polar external channel containing an H-bonding network of residues that extends to the bulk solvent water. Five separate mutations in one of these channel residues, Ser286 (Ser284 in Luc) of *L. mingrelica* luciferase (Figure 5), produced proteins whose bioluminescence spectra had maxima between 608 and 621 nm (*42*). In Luc, Ser284 is connected by an H-bonding network to Arg337 immediately through residue Glu311 (*25, 28*).

There are several ways that an Arg residue located near the benzothiazole ring of the emitter oxyluciferin might alter bioluminescence color. By anchoring the benzothiazole ring either through H-bonding interactions to the phenolic oxygen or through a cation$-\pi$ interaction, Arg218 may establish the normal yellow−green emission by restricting rotation about the C2−C2′ bond, a key feature of the TICT mechanism (*14*−*16*). It also is possible, however, that fixing the benzothiazole ring is important to the correct positioning of the oxyluciferin emitter near an essential nucleophilic residue, an important tenet of the color mechanism originally proposed by White (*8*). While we do believe Arg218 to be in a location similar to that shown in Figure 2, the data reported here do not allow us to favor one of these two positions.

According to the models discussed above (*27*−*29*), the putative LH_2 binding pocket is amphiphilic and contains ordered water molecules (*25, 28)*. We speculate that the normal binding of LH_2 displaces water from the amphiphilic site. Supporting data for the decreased exclusion of water from the LH_2 binding pockets of the Arg218 mutants were provided by the diminished ability of the Arg218 mutants to enhance the 440 nm fluorescence of L following the trend WT > R218K > R218Q ≈ R218A. The enhancement of the weak 440 nm fluorescence of L in Luc−L complexes is thought to reflect the diminished quenching by water (*13*). The TNS and L fluorescence experiments reported here support the contention that the changes at position 218 have altered the polarity of the LH_2/oxyluciferin binding site. It had previously been demonstrated that TNS binds at the LH_2 site of Luc and that the formation of a Luc−TNS complex was accompanied by intense fluorescence at 425 nm (*39*). This result was interpreted to mean that TNS was bound in a very hydrophobic environment (*39, 41*). The binding of TNS to mutant luciferases containing Ala at active site residues His245, Thr343, and Lys529 produced fluorescence results very similar to those with WT (data not shown). The complexes of TNS and the Arg218 mutants, however, gave fluorescence spectra with maxima at 430 nm for R218K and at 438 nm for R218Q and R218A. The red shifts in the fluorescence spectra imply that the LH_2 binding site of the R218K mutant is slightly less hydrophobic than that of WT and that the substrate sites of the Gln and Ala mutants are moderately less hydrophobic than WT (*41*). The mutations at position 218 may impair the ability of Luc to exclude water from excited-state oxyluciferin, thereby contributing to the red-shifted bioluminescence spectra produced by these enzymes.

After this project was completed and this report was prepared, an article appeared in which Viviani and Ohmyia described an investigation of bioluminescence color in two railroad worm (*Phrixothrix*) luciferases (*43*) (Figure 5). Citing our model as the basis for their investigation, they constructed R215S (R218 in Luc) mutants of *P. vivianii* and *P. hirtus* luciferases. Since no kinetics or fluorescence studies similar to those described here were reported, it is not possible to directly compare their study to our own. However, their major findings are relevant to this study. Specifically, the R215S mutations caused a red shift (from maximum at 548 to 585 nm) in the emission spectrum of the *P. vivianii* enzyme and had little effect on the emission (maximum at 623 nm) of the *P. hirtus* luciferase. The former result is similar to our measurements of 38 and 51 nm red shifts in the emission spectra of R218A and R218Q, respectively. Considering the properties of the small polar side chain of Ser (*44*), the color changes observed with the railroad worm enzyme would be expected in view of the above arguments for Luc. Generally, the conclusions of the two studies are mutually supportive. Currently, additional mutational studies are in progress to better understand the role of specific Luc active site residues in the determination of bioluminescence color.

ACKNOWLEDGMENT

We thank Monika Gruber and Marc Zimmer for helpful discussions; David Lloyd, John Thompson, and the DNA Sequencing Facility, Pfizer Inc., for providing DNA sequencing data; Justin Stroh and Linda Pezzullo for providing mass spectral data; and Evelyn Bamford for technical assistance.

REFERENCES

1. DeLuca, M. (1976) *Adv. Enzymol. Relat. Areas Mol. Biol. 44*, 37−68.
2. Wood, K. V. (1995) *Photochem. Photobiol. 62*, 662−673.
3. Wilson, T., and Hastings, J. W. (1998) *Annu. Rev. Cell. Dev. Biol. 14*, 197−230.
4. Contag, C. H., Spilman, S. D., Contag, P. R., Oshiro, M., Eames, B., Dennery, P., Stevenson, D. K., and Benaron, D. A. (1997) *Photochem. Photobiol. 66*, 523−531.
5. Kricka, L. J. (1995) *Anal. Chem. 67*, 499R−502R.
6. Price, R. L., Squirrell, D. J., and Murphy, M. J. (1998) *J. Clin. Ligand Assay 21*, 349−357.
7. Kricka, L. J. (2000) *Methods Enzymol. 305*, 333−345.
8. White, E. H., Rapaport, E., Seliger, H. H., and McElroy, W. D. (1971) *Bioorg. Chem. 1*, 92−122.
9. Seliger, H. H., and McElroy, W. D. (1960) *Arch. Biochem. Biophys. 88*, 136−141.
10. Rhodes, W. C., and McElroy, W. D. (1958) *J. Biol. Chem. 233*, 1528−1537.
11. McElroy, W. D., and Seliger, H. H. (1966) in *Molecular Architecture in Cell Physiology* (Hayashi, H., and Szent-Gyorgyi, I., Eds.) pp 63−79, Prentice-Hall, Englewood Cliffs, NJ.
12. Hastings, J. W. (1996) *Gene 173*, 5−11.
13. Morton, R. A., Hopkins, T. A., and Seliger, H. H. (1969) *Biochemistry 8*, 1598−1607.
14. McCapra, F., Gilfoyle, D. J., Young, D. W., Church, N. J., and Spencer, P. (1994) in *Bioluminescence and Chemiluminescence: Fundamentals and Applied Aspects* (Campbell, A. K., Kricka, L. J., and Stanley, P. E., Eds.) pp 387−391, John Wiley and Sons, Chichester.

15. McCapra, F. (1997) in *Bioluminescence and Chemiluminescence: Molecular Reporting with Photons* (Hastings, J. W., Kricka, L. J., and Stanley, P. E., Eds.) pp 7−15, John Wiley and Sons, Chichester.
16. McCapra, F. (2000) *Methods Enzymol. 305*, 3−47.
17. Wood, K. V., Lam, Y. A., Seliger, H. H., and McElroy, W. D. (1989) *Science 244*, 700−702.
18. Ye, L., Buck, L. M., Schaeffer, H. J., and Leach, F. R. (1997) *Biochim. Biophys. Acta 1339*, 39−52.
19. Viviani, V. R., Bechara, E. J. H., and Ohmiya, Y. (1999) *Biochemistry 38*, 8271−8279.
20. Viviani, V. R., Silva, A. C. R., Perez, G. L. O., Santelli, R. V., and Bechara, E. J. H. (1999) *Photochem. Photobiol. 70*, 254−260.
21. Suzuki, H., Kawarabayasi, Y., Kondo, J., Abe, T., Nishikawa, K., Kimura, S., Hashimoto, T., and Yamamoto, T. (1990) *J. Biol. Chem. 265*, 8681−8685.
22. Babbitt, P. C., Kenyon, G. L., Martin, B. M., Charest, H., Sylvestre, M., Scholten, J. D., Chang, K.-H., Liang, P.-H., and Dunaway-Mariano, D. (1992) *Biochemistry 31*, 5594−5604.
23. Chang, K.-H., Xiang, H., and Dunaway-Mariano, D. (1997) *Biochemistry 36*, 15650−15659.
24. Fontes, R., Ortiz, B., de Diego, A., Sillero, A., and Günther Sillero, M. A. (1998) *FEBS Lett. 438*, 190−194.
25. Conti, E., Franks, N. P., and Brick, P. (1996) *Structure 4*, 287−298.
26. Conti, E., Stachelhaus, T., Marahiel, M. A., and Brick, P. (1997) *EMBO J. 16*, 4174−4183.
27. Branchini, B. R., Magyar, R. A., Murtiashaw, M. H., Anderson, S. M., and Zimmer, M. (1998) *Biochemistry 37*, 15311−15319.
28. Franks, N. P., Jenkins, A., Conti, E., Lieb, W. R., and Brick, P. (1998) *Biophys. J. 75*, 2205−2211.
29. Sandalova, T. P., and Ugarova, N. N. (1999) *Biochemistry (Moscow) 64*, 1143−1150.
30. Imai, K., and Goto, T. (1988) *Agric. Biol. Chem. 52*, 2803−2809.
31. Branchini, B. R., Magyar, R. A., Murtiashaw, M. H., Anderson, S. M., Helgerson, L. C., and Zimmer, M. (1999) *Biochemistry 38*, 13223−13230.
32. Branchini, B. R., Murtiashaw, M. H., Magyar, R. A., and Anderson, S. M. (2000) *Biochemistry 39*, 5433−5440.
33. Thompson, J. F., Geoghegan, K. F., Lloyd, D. B., Lanzetti, A. J., Magyar, R. A., Anderson, S. M., and Branchini, B. R. (1997) *J. Biol. Chem. 272*, 18766−18771.
34. Branchini, B. R., Magyar, R. A., Marcantonio, K. M., Newberry, K. J., Stroh, J. G., Hinz, L. K., and Murtiashaw, M. H. (1997) *J. Biol. Chem. 272*, 19359−19364.
35. Dixon, M., and Webb, E. C. (1979) *Enzymes*, 3rd ed., pp 332−381, Academic Press, New York.
36. Denburg, J. L., Lee, R. T., and McElroy, W. D. (1969) *Arch. Biochem. Biophys. 131*, 381−391.
37. DeLuca, M., and McElroy, W. D. (1974) *Biochemistry 13*, 921−925.
38. Mode, V. A., and Sisson, D. H. (1974) *Anal. Chem. 46*, 200−203.
39. DeLuca, M. (1969) *Biochemistry 8*, 160−169.
40. Frydman, J. (1999) *Nat. Struct. Biol. 6*, 697−705.
41. McClure, W. O., and Edelman, G. M. (1966) *Biochemistry 5*, 1908−1919.
42. Arslan, T., Mamaev, S. V., Mamaeva, N. V., and Hecht, S. M. (1997) *J. Am. Chem. Soc. 119*, 10877−10884.
43. Viviani, V. R., and Ohmiya, Y. (2000) *Photochem. Photobiol. 72*, 267−271.
44. Creighton, T. E. (1993) *Proteins: structures and molecular properties*, 2nd ed., pp 139−169, W. H. Freeman and Company, New York.
45. Kraulis, P. J. (1991) *J. Appl. Crystallogr. 24*, 946−950.
46. DeWet, J. R., Wood, K. V., DeLuca, M., Helinski, D. R., and Subramani, S. (1987) *Mol. Cell. Biol. 7*, 725−737.
47. Sala-Newby, G. B., Thomson, C. M., and Campbell, A. K. (1996) *Biochem. J. 313*, 761−767.
48. Ohmiya, Y., Ohba, N., Toh, H., and Tsuji, F. I. (1995) *Photochem. Photobiol. 62*, 309−313.
49. Tatsumi, H., Kajiyama, N., and Nakano, E. (1992) *Biochim. Biophys. Acta 1131*, 161−165.
50. Cho, K. H. (1995) GenBank Z49891, direct submission.
51. Masuda, T., Tatsumi, H., and Nakano, E. (1989) *Gene 77*, 265−270.
52. Devine, J. H., Kutuzova, G. D., Green, V. A., Ugarova, N. N., and Baldwin, T. O. (1993) *Biochim. Biophys. Acta 1173*, 121−132.
53. Kajiyama, N., and Nakano, E. (1991) *Protein Eng. 4*, 691−693.
54. White, P. J., Squirrell, D. J., Arnaud, P., Lowe, C. R., and Murray, J. A. H. (1996) *Biochem. J. 319*, 343−350.

BI002246M